

---

# High-Dimensional Gaussian Process Regression with Soft Kernel Interpolation

---

Chris Camaño\*

California Institute of Technology  
ccamano@caltech.edu

Daniel Huang\*

San Francisco State University  
danehuang@sfsu.edu

## Abstract

We introduce *soft kernel interpolation* (SoftKI) designed for scalable Gaussian Process (GP) regression on high-dimensional datasets. Inspired by Structured Kernel Interpolation (SKI), which approximates a GP kernel via interpolation from a structured lattice, SoftKI approximates a kernel via softmax interpolation from a smaller number of learned interpolation (*i.e.*, inducing) points. By abandoning the lattice structure used in SKI-based methods, SoftKI separates the cost of forming an approximate GP kernel from the dimensionality of the data, making it well-suited for high-dimensional datasets. We demonstrate the effectiveness of SoftKI across various examples, and demonstrate that its accuracy exceeds that of other scalable GP methods when the data dimensionality is modest (around 10).

## 1 Introduction

Gaussian processes (GPs) are flexible function approximators based on Bayesian inference. However, there are scalability concerns. For a dataset comprising  $n$  data points, constructing the  $n \times n$  covariance matrix required for GP inference incurs a space complexity of  $\mathcal{O}(n^2)$ , and solving the associated linear system for exact posterior inference and hyperparameter optimization via direct methods requires  $\mathcal{O}(n^3)$  time complexity. These computational costs render exact GP inference challenging, even for modest  $n$ , though efforts have been made to accelerate exact GP inference (Wang et al., 2019; Gardner et al., 2021).

One approach to constructing scalable GP algorithms is based on *inducing points* (*e.g.*, see (Quinero-Candela and Rasmussen, 2005) and (Snelson and Ghahramani, 2005)). Intuitively, a set of inducing points forms a representative subset of the original dataset. Given  $m \ll n$  inducing points, we can form a low-rank approximation of the original GP kernel to construct an *approximate GP* which reduces the time complexity of posterior inference to  $\mathcal{O}(m^2n)$ . However, the limitation of using  $m \ll n$  inducing points means that the model may not accurately approximate the full kernel if the selected inducing points are not sufficiently representative of the entire dataset.

Another approach is based on *Structured Kernel Interpolation* (SKI) (Wilson and Nickisch, 2015) and its variants such as product kernel interpolation (Gardner et al., 2018) and Simplex-SKI (Kapoor et al., 2021). SKI approximates a GP kernel via interpolation from a pre-computed and dense rectilinear grid of inducing points. Structured interpolation enables fast matrix-vector multiplications (MVMs), which can be leveraged to scale inference by using the conjugate gradient (CG) method to solve for the inversion of the approximate kernel matrix. Importantly, SKI supports a larger number of inducing points than many other approximate GPs since it is applicable even when there is not low-rank structure in the true kernel. However, this approach also causes the time complexity of posterior inference to become dependent on the dimensionality  $d$  of the data (*e.g.*,  $\mathcal{O}(n4^d + m \log m)$  for a MVM in SKI and  $\mathcal{O}(d^2(n+m))$  for a MVM in Simplex-SKI). This motivates us to search for accurate and scalable GP regression algorithms that can scale to larger  $d$  while retaining the benefits of kernel interpolation.

In this paper, we introduce *soft kernel interpolation* (SoftKI), which combines aspects of inducing points and SKI to enable scalable GP regression on high-dimensional data sets. SoftKI retains SKI’s insight that a kernel can be well-approximated via interpolation. However, we opt to learn the locations of the interpolation points as in an inducing point approach.

---

\*Equal contribution.  
Preliminary work.

Our main observation is that while SKI can support large numbers of interpolation points, it uses them in a sparse manner—only a few interpolation points contribute to the interpolated value of any single data point. Consequently, we should still be able to interpolate successfully provided that we place enough inducing points in good locations relative to the dataset at hand, *i.e.*, learn their locations. The code can be found at <https://github.com/danehuang/softki>.

This change removes the explicit dependence of the cost of the method on the data dimensionality  $d$ , but at the cost of disrupting the structure of the kernel, motivating the need for an alternative inference method. We show how to recover efficient and accurate inference by interpolating from a softmax of  $m \ll n$  learned interpolation points, hence the name *soft kernel interpolation* (Section 4 and Section 4.2). The time complexity of posterior inference is  $\mathcal{O}(m^2n)$  and the space complexity is  $\mathcal{O}(mn)$  (Section 4.3). Additionally, SoftKI can leverage GPU acceleration and supports stochastic optimization for scalability. We evaluate SoftKIs on a variety of datasets from the UCI repository (Kelly et al., 2017) and show that it is more accurate in test Root Mean Square Error (RMSE) compared to popular scalable GP methods based on inducing points when the data dimensionality  $d$  is modest (around 10) and also scalable to larger  $d$  than methods based on SKI (Section 5). We also evaluate SoftKI on high-dimensional molecule datasets ( $d$  in the hundreds to thousands) and show its superior performance.

## 2 Background

**Notation.** We will write a list of vectors  $(x_i \in \mathbb{R}^d)_{1 \leq i \leq n}$  as the flattened length- $nd$  vector  $\mathbf{x}$  so that  $\mathbf{x}^T = (x_1^T \dots x_n^T)$ , *i.e.*,  $\mathbf{x}$  is a vector where indices  $d(i-1)$  to  $di$  exclusive is  $x_i$ . The notation  $f(\mathbf{x}) = (f(x_1) \dots f(x_N))^T$  maps a function  $f$  across a flattened list of vectors. Uppercase boldface letters denote matrices. We will sometimes use the notation  $[\cdot]_{ij}$  to define a matrix by defining its  $i$ th and  $j$ th entry. For example,  $\mathbf{A} = [g(i, j)]_{ij}$  defines a matrix  $\mathbf{A}$  whose  $i$ -th and  $j$ -th entry  $\mathbf{A}_{ij} = g(i, j)$ .

### 2.1 Gaussian processes

A (centered) *Gaussian process* (GP) is a random function  $f : \mathbb{R}^d \rightarrow \mathbb{R}$ . It has jointly Gaussian finite-dimensional distributions so that

$$f(\mathbf{x}) \sim \mathcal{N}(\mathbf{0}, \mathbf{K}_{\mathbf{xx}}) \quad (1)$$

for any  $\mathbf{x}$  where  $k : \mathbb{R}^d \times \mathbb{R}^d \rightarrow \mathbb{R}$  is a positive semi-definite function called a *kernel function*

and  $\mathcal{N}(\mathbf{0}, \mathbf{K}_{\mathbf{xx}})$  indicates a Gaussian distribution with mean  $\mathbf{0}$  and *kernel matrix*  $\mathbf{K}_{\mathbf{xx}} = [k(x_i, x_j)]_{ij}$  (also called covariance matrix).

To perform GP regression on the labeled dataset  $\{(x_i, y_i) : x_i \in \mathbb{R}^d, y_i \in \mathbb{R}, 1 \leq i \leq n\}$ , we assume the data is generated as follows:

$$\begin{aligned} f(\mathbf{x}) &\sim \mathcal{N}(\mathbf{0}, \mathbf{K}_{\mathbf{xx}}) && \text{(GP)} \\ \mathbf{y} | f(\mathbf{x}) &\sim \mathcal{N}(f(\mathbf{x}), \beta^2 \mathbf{I}) && \text{(likelihood)} \end{aligned}$$

where  $f$  is a function sampled from a GP and each observation  $y_i$  is  $f$  evaluated at  $x_i$  perturbed by independent and identically distributed (i.i.d.) Gaussian noise with zero mean and variance  $\beta^2$ . The posterior predictive distribution has the closed-form solution (Rasmussen and Williams, 2005)

$$\begin{aligned} p(f(*) | \mathbf{y}) &= \mathcal{N}(\mathbf{K}_{*\mathbf{x}}(\mathbf{K}_{\mathbf{xx}} + \mathbf{\Lambda})^{-1}\mathbf{y}, \\ &\quad \mathbf{K}_{**} - \mathbf{K}_{*\mathbf{x}}(\mathbf{K}_{\mathbf{xx}} + \mathbf{\Lambda})^{-1}\mathbf{K}_{\mathbf{x}*}) \end{aligned} \quad (2)$$

where  $\mathbf{\Lambda} = \beta^2 \mathbf{I}$ . Using standard direct methods, the time complexity of inference is  $\mathcal{O}(n^3)$  which is the complexity of solving the system of linear equations in  $n$  variables

$$(\mathbf{K}_{\mathbf{xx}} + \mathbf{\Lambda})\alpha = \mathbf{y} \quad (3)$$

for  $\alpha$  so that the posterior mean (2) is  $\mathbf{K}_{*\mathbf{x}}\alpha$ .

A GP’s *hyperparameters*  $\theta$  include the noise  $\beta^2$  and other parameters such as those involved in the definition of a kernel such as its *lengthscale*  $\ell$  and *scale*  $\sigma$ . Thus  $\theta = (\beta, \ell, \sigma)$ . The hyperparameters can be set by maximizing the log-marginal likelihood of a GP

$$\log p(\mathbf{y}; \theta) = \mathcal{N}(\mathbf{y} | \mathbf{0}, \mathbf{K}_{\mathbf{xx}}(\theta) + \mathbf{\Lambda}(\theta)) \quad (4)$$

where  $\mathcal{N}(\cdot | \mu, \mathbf{\Sigma})$  is notation for the probability density function (PDF) of a Gaussian distribution with mean  $\mu$  and covariance  $\mathbf{\Sigma}$  and we have explicitly indicated the dependence of  $\mathbf{K}_{\mathbf{xx}}$  and  $\mathbf{\Lambda}$  on  $\theta$ . For simplicity, we will abbreviate  $\log p(\mathbf{y}; \theta) = \log p(\mathbf{y})$  and leave the dependence on hyperparameters implicit.

### 2.2 Sparse Gaussian Process Regression.

Many scalable GP methods address the high computational cost of GP inference by approximating the kernel using a Nyström method (Williams and Seeger, 2000). This approach involves selecting a smaller set of  $m$  inducing points,  $\mathbf{z} \subset \mathbf{x}$ , to serve as representatives for the complete dataset. The original  $n \times n$  kernel  $\mathbf{K}_{\mathbf{xx}}$  is then approximated as:

$$\mathbf{K}_{\mathbf{xx}} \approx \mathbf{K}_{\mathbf{zx}}\mathbf{K}_{\mathbf{zz}}^{-1}\mathbf{K}_{\mathbf{zx}} \quad (5)$$

leading to an overall inference complexity of  $\mathcal{O}(m^2n)$ .

Over the last two decades, Nyström approximation for GP kernels has been refined and adapted in various ways, with many improvements driven by a theoretical re-characterization of inducing points as *inducing variables* and the limitations of the Nyström approximation as a standalone approximation of the true covariance  $\mathbf{K}_{\mathbf{xx}}$  (Quinero-Candela and Rasmussen, 2005). These ideas were crystallized into the widely used SGPR method (Titsias, 2009), which combines Nyström GP kernel approximation with a variational optimization process. To perform SGPR, we use the following generative process:

$$\begin{aligned} \begin{pmatrix} u \\ f(\mathbf{x}) \end{pmatrix} &\sim \mathcal{N}\left(\begin{pmatrix} \mathbf{0} \\ \mathbf{0} \end{pmatrix}, \begin{pmatrix} \mathbf{K}_{\mathbf{zz}} & \mathbf{K}_{\mathbf{zx}} \\ \mathbf{K}_{\mathbf{zx}} & \mathbf{K}_{\mathbf{xx}} \end{pmatrix}\right) & \text{(SGPR)} \\ \mathbf{y} | f(\mathbf{x}) &\sim \mathcal{N}(f(\mathbf{x}), \Lambda) & \text{(likelihood)} \end{aligned}$$

where  $u$  are *inducing variables* and  $\mathbf{z}$  is a set of *inducing points*. We will abbreviate  $f(\mathbf{x}) = f$ . Observe that  $f \sim \mathcal{N}(\mathbf{0}, \mathbf{K}_{\mathbf{xx}})$  so that a SGPR reduces to GP regression after marginalizing out the inducing variables  $u$ . In SGPR, inference is directly performed with the inducing variables  $u$  since marginalization would lead to an expensive computation. Consequently, we need a procedure for selecting the inducing points  $\mathbf{z}$ .

Towards this end, (Titsias, 2009) introduces a variational distribution  $q(f, u) = p(f | u)q(u)$  and solves for the  $q(u)$  that minimizes the KL divergence  $\text{KL}(q(f, u) || p(f, u | \mathbf{y}))$ . The optimal  $q(u)$  is

$$q(u) = \mathcal{N}(\mathbf{K}_{\mathbf{zz}} \mathbf{C}^{-1} \mathbf{K}_{\mathbf{zx}} \Lambda^{-1} \mathbf{y}, \mathbf{K}_{\mathbf{zz}} \mathbf{C}^{-1} \mathbf{K}_{\mathbf{zz}}) \quad (6)$$

where  $\mathbf{C} = \mathbf{K}_{\mathbf{zz}} + \mathbf{K}_{\mathbf{zx}} \Lambda^{-1} \mathbf{K}_{\mathbf{zx}}$ . This maximizes the evidence lower bound (ELBO)

$$\begin{aligned} \text{ELBO}(q(f, u)) &= \log p(\mathbf{y}) - \text{KL}(q(f, u) || p(f, u | \mathbf{y})) \\ &= \log \mathcal{N}(\mathbf{y} | \mathbf{0}, \mathbf{Q}_{\mathbf{xx}}^z + \Lambda) - \frac{1}{2} \text{Tr}(\mathbf{K}_{\mathbf{xx}} - \mathbf{Q}_{\mathbf{xx}}^z) \end{aligned} \quad (7)$$

where  $\mathbf{Q}_{\mathbf{xx}}^z = \mathbf{K}_{\mathbf{zx}} \mathbf{K}_{\mathbf{zz}}^{-1} \mathbf{K}_{\mathbf{zx}}$  is a Nyström approximation of  $\mathbf{K}_{\mathbf{xx}}$ . Since the ELBO is a lower bound on the log-marginal likelihood  $\log p(\mathbf{y})$ , we can maximize the ELBO via gradient based optimization as a proxy for maximizing  $\log p(\mathbf{y})$  to learn the location of the inducing points  $\mathbf{z}$  by treating it as a GP hyperparameter, *i.e.*,  $\theta = (\beta, \ell, \sigma, \mathbf{z})$ . The time complexity of computing the ELBO is  $\mathcal{O}(m^2 n)$ .

Given learned inducing points, the posterior predictive distribution  $q(f | *)$  has closed form

$$\begin{aligned} q(f | *) | \mathbf{y} &= \mathcal{N}(f | *) | \mathbf{K}_{*\mathbf{z}} \mathbf{C}^{-1} \mathbf{K}_{\mathbf{zx}} \Lambda^{-1} \mathbf{y}, \\ &\quad \mathbf{K}_{**} - \mathbf{K}_{*\mathbf{z}} (\mathbf{K}_{\mathbf{zz}}^{-1} - \mathbf{C}^{-1}) \mathbf{K}_{\mathbf{z}*}. \end{aligned} \quad (8)$$

The time complexity of posterior inference is  $\mathcal{O}(m^2 n + m^3)$  since it requires solving

$$\mathbf{C} \alpha = \mathbf{K}_{\mathbf{zx}} \Lambda^{-1} \mathbf{y} \quad (9)$$

for  $\alpha$  which is dominated by forming  $\mathbf{C}$ .

### 2.3 Structured Kernel Interpolation.

SKI approaches scalable GP regression by approximating a large covariance matrix  $\mathbf{K}_{\mathbf{xx}}$  by interpolating from cleverly chosen inducing points. In particular, SKI makes the approximation

$$\tilde{\mathbf{Q}}_{\mathbf{xx}'}^z = \mathbf{W}_{\mathbf{xz}} \mathbf{K}_{\mathbf{zz}} \mathbf{W}_{\mathbf{zx}'} \quad (10)$$

$$= (\mathbf{W}_{\mathbf{xz}} \mathbf{K}_{\mathbf{zz}}) \mathbf{K}_{\mathbf{zz}}^{-1} (\mathbf{K}_{\mathbf{zz}} \mathbf{W}_{\mathbf{zx}'}) \quad (11)$$

$$= \hat{\mathbf{K}}_{\mathbf{xz}} \mathbf{K}_{\mathbf{zz}}^{-1} \hat{\mathbf{K}}_{\mathbf{zx}'} \quad (12)$$

$$\approx \mathbf{K}_{\mathbf{xx}'} \quad (13)$$

where  $\mathbf{W}_{\mathbf{xz}}$  is a sparse matrix of interpolation weights,  $\hat{\mathbf{K}}_{\mathbf{xz}} = \mathbf{W}_{\mathbf{xz}} \mathbf{K}_{\mathbf{zz}}$ , and  $\hat{\mathbf{K}}_{\mathbf{zx}'} = \mathbf{K}_{\mathbf{zz}} \mathbf{W}_{\mathbf{zx}'}$ . The posterior predictive distribution is then the standard GP posterior predictive

$$\begin{aligned} p(f | *) | \mathbf{y} &\approx \mathcal{N}(\mathbf{K}_{**} (\tilde{\mathbf{Q}}_{\mathbf{xx}}^z + \Lambda)^{-1} \mathbf{y}, \\ &\quad \mathbf{K}_{**} - \mathbf{K}_{**} (\tilde{\mathbf{Q}}_{\mathbf{xx}}^z + \Lambda)^{-1} \mathbf{K}_{**}) \end{aligned} \quad (14)$$

where  $\mathbf{K}_{\mathbf{xx}}$  is replaced with  $\tilde{\mathbf{Q}}_{\mathbf{xx}}^z$ . SKI uses linear CG to solve the linear system

$$(\tilde{\mathbf{Q}}_{\mathbf{xx}}^z + \Lambda) \alpha = \mathbf{y} \quad (15)$$

for  $\alpha$ . Since the time complexity of CG depends on access to fast MVMs, SKI makes two design choices that are compatible with CG. First, SKI uses cubic interpolation (Keys, 1981) weights so that  $\mathbf{W}_{\mathbf{xz}}$  has four non-zero entries in each row, *i.e.*,  $\mathbf{W}_{\mathbf{xz}}$  is sparse. Second, SKI chooses the inducing points  $\mathbf{z}$  to be on a fixed rectilinear grid in  $\mathbb{R}^d$  which induces multilevel Toeplitz structure in  $\mathbf{K}_{\mathbf{zz}}$  if  $k(x, y)$  is a stationary kernel.

Putting the two together, the resulting  $\tilde{\mathbf{Q}}_{\mathbf{xx}}^z$  is a structured kernel which enables fast MVMs. If we wish to have  $k$  distinct inducing points for each dimension, the grid will contain  $m = k^d$  inducing points leading to a total complexity of GP inference of  $\mathcal{O}(n 4^d + m \log(m)) = \mathcal{O}(n 4^d + dk^d \log(k))$  since there are  $\mathcal{O}(4^d)$  nonzero entries per row of  $\mathbf{W}_{\mathbf{xz}}$  and a MVM with a Toeplitz structured kernel like  $\mathbf{K}_{\mathbf{zz}}$  can be done in  $\mathcal{O}(m \log m)$  time via a Fast Fourier Transform (FFT) (Wilson, 2014). Thus, for low dimensional problems, SKI can provide significant speedups compared to vanilla GP inference and supports a larger number of inducing points compared to SGPR.

### 3 Related work

Beyond SGPR and vanilla SKI, a wide range of approximate GP models and variants have been developed that align closely with SoftKI.

Building on SGPR, Stochastic Variational Gaussian Processes (SVGP) (Hensman et al., 2013) extends the

optimization process used for SGPR to use stochastic variational inference. This further reduces the computational cost of GP inference to  $\mathcal{O}(m^3)$  since optimization is now over a variational distribution on  $\mathbf{z}$ , rather than the full posterior. Importantly SVGP is highly scalable to GPUs since its optimization strategy is amenable to minibatch optimization procedures.

### Variants of Structured Kernel Interpolation.

While SKI can provide significant speedups over vanilla GP inference, its scaling restricts its usage to low-dimensional settings where  $4^d < n$ . To address this, (Gardner et al., 2018) introduced SKIP, which optimizes SKI by expressing a  $d$ -dimensional kernel as a product of  $d$  one-dimensional kernels. This reduces MVM costs from  $\mathcal{O}(dk^d \log k)$  to  $\mathcal{O}(dm \log m)$ , using  $m$  grid points per component kernel instead of  $k^d$ . However, SKIP is limited to dimensions 10 to 30 for large datasets, as it requires substantial memory and may suffer from low-rank approximation errors.

Recent work on improving the scaling properties of SKI has been focused on efficient incorporation of simplicial interpolation, which when implemented carefully in the case of Simplex-GP (Kapoor et al., 2021) and Sparse grid GP (Yadav et al., 2023) can reduce the cost of a single MVM with an  $\mathbf{W}_{\mathbf{z}\mathbf{z}}$  down to  $\mathcal{O}(nd^2)$ . These methods differ in the grid construction used for interpolation with Simplex-SKI opting for a permutohedral lattice (Adams et al., 2010), while sparse grid-GP uses sparse grids and a bespoke recursive MVM algorithm, leading to  $\mathbf{K}_{\mathbf{z}\mathbf{z}}$  MVM costs of  $\mathcal{O}(d^2(n+m))$  and  $\mathcal{O}(m(\log m)^d)$  respectively. While both of these methods greatly improve the scaling of SKI, they still feature a problematic dependency on  $d$  limiting their extension to arbitrarily large datasets.

## 4 Method

In this section, we introduce SoftKI (Algorithm 1). To construct a SoftKI, we will take the same starting point as SKI, namely that

$$\tilde{\mathbf{Q}}_{\mathbf{x}\mathbf{x}'}^{\mathbf{z}} = \mathbf{W}_{\mathbf{x}\mathbf{z}} \mathbf{K}_{\mathbf{z}\mathbf{z}} \mathbf{W}_{\mathbf{z}\mathbf{x}'} \quad (16)$$

can be used as an approximation of  $\mathbf{K}_{\mathbf{x}\mathbf{x}}$ . However, we will deviate in that we will abandon the structure given by a lattice and opt to learn the locations of the interpolation points  $\mathbf{z}$  instead. This raises several issues. First, we revisit the choice of interpolation because we have changed the locations of the interpolation points (Section 4). Second, we require an efficient procedure for learning the inducing points (Section 4.2). Third, we require an alternative route to recover a scalable GP since our approach removes structure in the kernel that was used in SKI for efficient inference (Section 4.3).

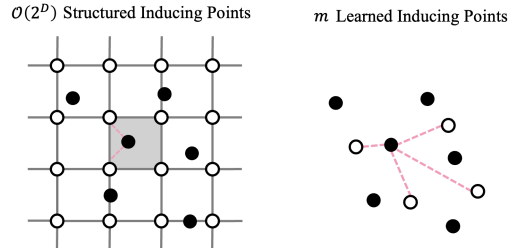


Figure 1: Comparison of interpolation procedure for linear interpolation to the two nearest grid points during SKI and softmax interpolation during SoftKI. Here white points  $\circ$  indicate inducing points  $z_i \in \mathbf{z}$  and black points  $\bullet$  are data points  $x_i \in \mathbf{x}$ .

### 4.1 Soft Kernel Interpolation

Whereas a cubic (or higher-order) interpolation scheme is natural in SKI when using a static lattice structure, our situation is different since the locations of the interpolation points are dynamic. In particular, we would ideally want our interpolation scheme to have the flexibility to adjust the contributions of inducing points used to interpolate a kernel value in a data-dependent manner. To accomplish this, we propose *softmax interpolation weights*.

**Definition 4.1** (Softmax interpolation weights). Define *softmax interpolation weights* as the following matrix

$$\mathbf{W}_{\mathbf{x}\mathbf{z}} = \left[ \frac{\exp(-\|x_i - z_j\|)}{\sum_{k=1}^m \exp(-\|x_i - z_k\|)} \right]_{ij}. \quad (17)$$

Since a softmax can be interpreted as a probability distribution, we can view SoftKI as interpolating from a probabilistic mixture of inducing points. Softmax interpolation ensures that each input point  $x_i$  is interpolated from all inducing points, with an exponential weighting favoring closer points. As a result, we obtain a matrix  $\mathbf{W}_{\mathbf{x}\mathbf{z}}$  where each row  $\mathbf{W}_{x_i\mathbf{z}}$  represents the softmax interpolation weights between a single point  $x_i$  and all  $m$  inducing points (Figure 1). Since softmax interpolation continuously assigns weights over each inducing point for each  $x_i$ , the resulting  $\mathbf{W}_{\mathbf{x}\mathbf{z}}$  matrix is not strictly sparse. However, as  $d$  increases the weights for distant points become negligible. This leads to an effective sparsity, with each  $x_i$  predominantly influenced only by its nearest inducing points during reconstruction of  $\mathbf{K}_{\mathbf{x}\mathbf{x}}$ .

### 4.2 Learning Inducing Points

Similar to a SGPR, we can treat the inducing points  $\mathbf{z}$  as hyper parameters of a GP and learn them by optimizing an appropriate objective. We propose optimiz-

**Algorithm 1** SoftKI Regression. The procedure `kmeans` performs k-means clustering, `batch` splits the dataset into batches, and `softmax_interpolation` produces a softmax interpolation matrix (see Section 4).

**Require:** SoftKI GP hyperparameters  $\theta = (\ell, \sigma, \mathbf{z}^{(M \times d)})$ , consisting of kernel lengthscale  $\ell$ , output scale  $\sigma$ , and inducing points  $\mathbf{z}$ . Kernel function  $k(x, y)$ .

**Require:** Dataset  $(\mathbf{x}^{(N \times d)}, \mathbf{y}^{(N \times 1)})$ .

**Require:** Optimization hyperparameters: batch size  $B$ , fixed noise  $\Lambda$ , and learning rate  $\eta$ .

**Ensure:** Learned SoftKI coefficients  $\alpha$ .

```

1:  $\mathbf{z} \leftarrow \text{kmeans}(\mathbf{x}, M)$ 
2: for  $i = 1$  to epochs do
3:   for  $b$  in batch $(\mathbf{x}, \mathbf{y}, B)$  do
4:      $\mathbf{W}_{\mathbf{x}_b \mathbf{z}} \leftarrow \text{softmax\_interpolation}(\mathbf{x}_b, \mathbf{z})$ 
5:      $\mathbf{K}_{\mathbf{z}\mathbf{z}} \leftarrow k(\mathbf{z}, \mathbf{z})$ 
6:      $\tilde{\mathbf{Q}}_{bb}^{\mathbf{z}} \leftarrow \mathbf{W}_{\mathbf{x}_b \mathbf{z}} \mathbf{K}_{\mathbf{z}\mathbf{z}} \mathbf{W}_{\mathbf{x}_b \mathbf{z}}^\top$ 
7:      $\theta \leftarrow \theta + \eta \nabla_{\theta} \log \tilde{p}(\mathbf{y}_b; \tilde{\mathbf{Q}}_{bb}^{\mathbf{z}} + \Lambda)$ 
8:   end for
9: end for
10:  $\mathbf{W}_{\mathbf{x}\mathbf{z}} \leftarrow \text{softmax\_interpolation}(\mathbf{x}, \mathbf{z})$ 
11:  $\mathbf{U}_{\mathbf{z}\mathbf{z}} \mathbf{U}_{\mathbf{z}\mathbf{z}}^\top \leftarrow \text{cholesky}(\mathbf{K}_{\mathbf{z}\mathbf{z}})$ 
12:  $\mathbf{Q}, \mathbf{R} \leftarrow \text{QR} \left( \begin{pmatrix} \Lambda^{-1/2} \mathbf{W}_{\mathbf{x}\mathbf{z}} \mathbf{K}_{\mathbf{z}\mathbf{z}} \\ \mathbf{U}_{\mathbf{z}\mathbf{z}} \end{pmatrix} \right)$ 
13:  $\alpha \leftarrow \mathbf{R}^{-1} \mathbf{Q}^\top \begin{pmatrix} \Lambda^{-1/2} \mathbf{y} \\ 0 \end{pmatrix}$ 
14: return  $\alpha$ 

```

ing the marginal log likelihood  $\log p(\mathbf{y})$  for a SoftKI which has closed form solution

$$\log p(\mathbf{y}) = \log \mathcal{N}(\mathbf{y} | \mathbf{0}, \tilde{\mathbf{Q}}_{\mathbf{x}\mathbf{x}}^{\mathbf{z}} + \Lambda). \quad (18)$$

Each evaluation of  $\log p(\mathbf{y})$  has time complexity  $\mathcal{O}(m^2 n)$  and space complexity  $\mathcal{O}(mn)$  where  $m$  is the number of interpolation points. However, this is tractable to compute only when  $m \ll n$  because  $\tilde{\mathbf{Q}}_{\mathbf{x}\mathbf{x}}^{\mathbf{z}}$  is low-rank. We thus propose to learn  $m \ll n$  inducing points by maximizing  $\log p(\mathbf{y})$  with a method based on gradient descent. In our experience a direct implementation of (18) is prone to numerical instability since it is possible for  $\tilde{\mathbf{Q}}_{\mathbf{x}\mathbf{x}}^{\mathbf{z}} + \Lambda$  to only be approximately psd (See Appendix B.1).

**Hutchinson’s Pseudoloss.** To address this problem, we compute a pseudo-marginal log likelihood  $\log \tilde{p}(\mathbf{y}; \theta)$  following (Maddox et al., 2022), which was originally used to stabilize GP regression in low precision settings. The main idea is to construct a  $\log \tilde{p}(\mathbf{y}; \theta)$  such that  $\nabla_{\theta} \log \tilde{p}(\mathbf{y}; \theta) \approx \nabla_{\theta} \log p(\mathbf{y}; \theta)$ . In this way, a gradient-based optimization scheme can still optimize the GP hyperparameters  $\theta$  as if the exact marginal log likelihood was used.

Let  $\Sigma_{\theta} = \tilde{\mathbf{Q}}_{\mathbf{x}\mathbf{x}}^{\mathbf{z}}(\theta) + \Lambda(\theta)$  where we have explicitly indicated the dependence on the GP hyperparameters  $\theta$ .

**Definition 4.2** (Hutchinson Pseudoloss). The *Hutchinson Pseudoloss* is defined as

$$\log \tilde{p}(\mathbf{y}; \theta) = \frac{1}{2L} \sum_{j=1}^L \mathbf{a}_j^T (\Sigma_{\theta} \mathbf{b}_j) - \frac{1}{2} \mathbf{b}_0^T \Sigma_{\theta} \mathbf{b}_0 \quad (19)$$

where  $\mathbf{a}_i$  are Gaussian random vectors normalized to have unit length, and  $\mathbf{b}_1, \dots, \mathbf{b}_L$  are solutions to the equations

$$\Sigma_{\theta}(\mathbf{b}_0 \mathbf{b}_1 \dots \mathbf{b}_n) = (\mathbf{y} \mathbf{a}_1 \dots \mathbf{a}_M). \quad (20)$$

The gradient of  $\log \tilde{p}(\mathbf{y}; \theta)$  w.r.t. the hyperparameters  $\theta$  is

$$\begin{aligned} \nabla_{\theta} \log \tilde{p}(\mathbf{y}; \theta) &= \frac{1}{2L} \sum_{j=1}^L \mathbf{a}_j^T (\nabla_{\theta} \Sigma_{\theta} \mathbf{b}_j) - \frac{1}{2} \mathbf{b}_0^T (\nabla_{\theta} \Sigma_{\theta} \mathbf{b}_0) \quad (21) \\ &\approx \frac{1}{2} \text{Tr}(\Sigma_{\theta}^{-1} (\nabla_{\theta} \Sigma_{\theta})) - \frac{1}{2} (\Sigma_{\theta}^{-1} \mathbf{y})^T (\nabla_{\theta} \Sigma_{\theta}) (\Sigma_{\theta}^{-1} \mathbf{y}) \quad (22) \end{aligned}$$

$$= \nabla_{\theta} \log p(\mathbf{y}; \theta) \quad (23)$$

so that it is approximately equivalent to the gradient of  $\log p(\mathbf{y})$  w.r.t. the hyperparameters estimated with Hutchinson’s trace estimator (Girard, 1989; Hutchinson, 1989; Gibbs and MacKay, 1996).

**Stochastic optimization.** For further stability, we perform minibatch gradient descent on the Hutchinson pseudoloss (see line 7 of Algorithm 1). We emphasize that we are performing stochastic gradient descent and not stochastic variational inference as in SVGP (Hensman et al., 2013). In particular, we do not define a distribution on  $\mathbf{z}$  nor make a variational approximation. Our experiments (Section 5) show that this approach works well in practice.

### 4.3 Posterior Inference

Because  $\tilde{\mathbf{Q}}_{\mathbf{x}\mathbf{x}}^{\mathbf{z}}$  is low-rank, we can use the matrix inversion lemma to rewrite the posterior predictive of SoftKI as

$$\begin{aligned} p(f_{\mathbf{z}}(*) | \mathbf{y}) &= \mathcal{N}(\hat{\mathbf{K}}_{*\mathbf{z}} \hat{\mathbf{C}}^{-1} \hat{\mathbf{K}}_{\mathbf{z}\mathbf{z}} \Lambda^{-1} \mathbf{y}, \tilde{\mathbf{Q}}_{**}^{\mathbf{z}} - \\ &\quad \tilde{\mathbf{Q}}_{*\mathbf{x}}^{\mathbf{z}} (\Lambda^{-1} - \Lambda^{-1} \hat{\mathbf{K}}_{\mathbf{z}\mathbf{z}} \hat{\mathbf{C}}^{-1} \hat{\mathbf{K}}_{\mathbf{z}\mathbf{x}} \Lambda^{-1} \tilde{\mathbf{Q}}_{\mathbf{x}\mathbf{x}}^{\mathbf{z}} \Lambda^{-1}) \tilde{\mathbf{Q}}_{\mathbf{x}*}^{\mathbf{z}}) \quad (24) \end{aligned}$$

where  $\hat{\mathbf{C}} = \mathbf{K}_{\mathbf{z}\mathbf{z}} + \hat{\mathbf{K}}_{\mathbf{z}\mathbf{x}} \Lambda^{-1} \hat{\mathbf{K}}_{\mathbf{x}\mathbf{z}}$  (see Appendix A). To perform posterior mean inference, we solve

$$\hat{\mathbf{C}} \alpha = \hat{\mathbf{K}}_{\mathbf{z}\mathbf{x}} \Lambda^{-1} \mathbf{y} \quad (25)$$

for weights  $\alpha$ . Note that this is the posterior mean of a SGPR with  $\mathbf{C}$  replaced with  $\hat{\mathbf{C}}$  and  $\mathbf{K}_{\mathbf{xz}}$  replaced with  $\hat{\mathbf{K}}_{\mathbf{xz}}$ . Moreover, note that  $\hat{\mathbf{C}}$  is  $\mathbf{C}$  with  $\mathbf{K}_{\mathbf{zz}}$  replaced with  $\hat{\mathbf{K}}_{\mathbf{zz}}$ . Since  $\hat{\mathbf{C}}$  is a  $m \times m$  matrix, the solution of the system of linear equations has time complexity  $\mathcal{O}(m^3)$ . The formation of  $\hat{\mathbf{C}}$  requires the multiplication of a  $m \times n$  matrix with a  $n \times m$  matrix which has time complexity  $\mathcal{O}(m^2n)$ . Thus the complexity of SoftKI posterior mean inference is  $\mathcal{O}(m^2n)$  since it is dominated by the formation of  $\hat{\mathbf{C}}$ .

**Solving with QR.** Unfortunately, solving (25) for  $\alpha$  can be numerically unstable. (Foster et al., 2009) introduce a stable QR solver approach for a Subset of Regressors (SoR) GP (Smola and Bartlett, 2000) which we adapt to a SoftKI.

Define a matrix

$$\mathbf{A} = \begin{pmatrix} \Lambda^{-1/2} \hat{\mathbf{K}}_{\mathbf{xz}} \\ \mathbf{U}_{\mathbf{zz}} \end{pmatrix} \quad (26)$$

where  $\mathbf{U}_{\mathbf{zz}} \mathbf{U}_{\mathbf{zz}}^\top = \mathbf{K}_{\mathbf{zz}}$  is the Cholesky decomposition of  $\mathbf{K}_{\mathbf{zz}}$  so that

$$\mathbf{A}^\top \mathbf{A} = \hat{\mathbf{K}}_{\mathbf{zx}} \Lambda^{-1} \hat{\mathbf{K}}_{\mathbf{xz}} + \mathbf{K}_{\mathbf{zz}} = \hat{\mathbf{C}}. \quad (27)$$

Let  $\mathbf{QR} = \mathbf{A}$  be the the QR decomposition of  $\mathbf{A}$  so that  $\mathbf{Q}$  is a  $(n+m) \times m$  orthogonal matrix and  $\mathbf{R}$  is  $m \times m$  right triangular matrix. Then

$$\alpha = \hat{\mathbf{C}}^{-1} \hat{\mathbf{K}}_{\mathbf{zx}} \Lambda^{-1} \mathbf{y} \quad (28)$$

$$= ((\mathbf{QR})^\top (\mathbf{QR}))^{-1} (\mathbf{QR})^\top \begin{pmatrix} \Lambda^{-1/2} \mathbf{y} \\ 0 \end{pmatrix} \quad (29)$$

$$= \mathbf{R}^{-1} \mathbf{Q}^\top \begin{pmatrix} \Lambda^{-1/2} \mathbf{y} \\ 0 \end{pmatrix} \quad (30)$$

is a solution to  $\hat{\mathbf{C}} \alpha = \hat{\mathbf{K}}_{\mathbf{zx}} \Lambda^{-1} \mathbf{y}$ . We thus solve  $\mathbf{R} \alpha = \mathbf{Q}^\top \begin{pmatrix} \Lambda^{-1/2} \mathbf{y} \\ 0 \end{pmatrix}$  for  $\alpha$ . For additional experiments demonstrating the inability of other linear solvers to offer comparable accuracy to the QR-stabilized solve detailed in this section, see Appendix B.3.

## 5 Experiments

We compare the performance of SoftKIs against popular scalable GPs on selected data sets from the UCI data set repository (Kelly et al., 2017), a common GP benchmark (Section 5.1). Next, we test SoftKIs on high-dimensional molecule data sets from the domain of computational chemistry (Section 5.2). Finally we explore the role of noise in a SoftKI and discuss best practices (Section 5.3).

### 5.1 Benchmark on UCI Regression

We evaluate the efficacy of a SoftKI against other scalable GP methods on data sets of varying size  $n$  and

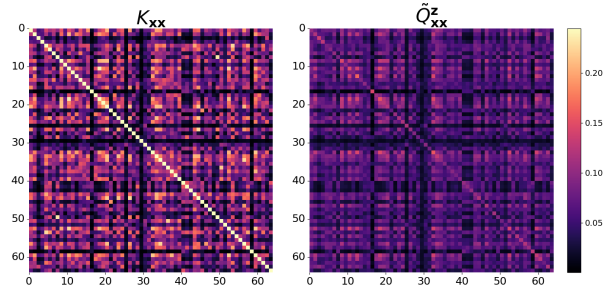


Figure 2: Comparison of the first 64 samples of the exact GP kernel ( $\mathbf{K}_{\mathbf{xx}}$ ) evaluated on the `elevators` test dataset versus the approximate GP kernel ( $\hat{\mathbf{Q}}_{\mathbf{xx}}^z$ ) learned by a SoftKI after 50 epochs of training.

data dimensionality  $d$  from the UCI repository (Kelly et al., 2017). We choose SGPR and SVGP as two scalable GP methods since these methods can be applied in a relatively blackbox fashion, and thus, can be applied to many data sets.

**Hardware details.** We run all experiments on a single Nvidia RTX 3090 GPU which has 24Gb of VRAM. A GPU with more VRAM can support larger datasets. Our machine uses an Intel i9-10900X CPU at 3.70GHz with 10 cores. This primarily affects the timing of SoftKI and SVGP which use batched hyperparameter optimization, and thus, move data on and off the GPU more frequently than SGPR.

**Experiment details.** For this experiment, we split the data set into 0.9 for training and 0.1 for testing. We standardize the data to have mean 0 and standard deviation 1 using the training data set. We use a radial basis function (RBF) kernel with a single learnable lengthscale for all dimensions and a learnable output scale. We choose  $m = 512$  inducing points for SoftKI. Following (Wang et al., 2019), we use  $m = 512$  for SGPR and  $m = 1024$  for SVGP. We learn model hyperparameters for SoftKI by maximizing the marginal log likelihood, and for SGPR and SVGP by maximizing the ELBO. However, we opt to not learn the noise  $\beta^2$  for SoftKI instead fixing the value as  $\beta^2 = 0.001$  which is explained further in Section 5.3.

We perform 50 iterations of training using the Adam optimizer (Kingma and Ba, 2014) for all methods with a learning rate of  $\eta = 0.01$ . The learning rate for SGPR is  $\eta = 0.1$  since we are not performing batching. We use a default implementation of SGPR and SVGP from GPyTorch. For SoftKI and SVGP, we use a minibatch size of 1024. We report the average test RMSE and hyperparameter optimization time for each method across three seeds. A visualization of the learned kernel  $\hat{\mathbf{Q}}_{\mathbf{xx}}^z$  for the `elevators` dataset is given

	n	d	SoftKI-512	SGPR-512	SVGP-1024
3droad	391386	3	0.605 ± 0.0	-	<b>0.496 ± 0.001</b>
Kin40k	36000	8	0.237 ± 0.008	0.205 ± 0.008	<b>0.192 ± 0.006</b>
Protein	41157	9	<b>0.649 ± 0.01</b>	0.66 ± 0.009	0.659 ± 0.008
Houseelectric	1844352	11	<b>0.064 ± 0.001</b>	-	0.071 ± 0.0
Bike	15641	17	<b>0.204 ± 0.006</b>	0.284 ± 0.002	0.268 ± 0.003
Elevators	14939	18	<b>0.389 ± 0.01</b>	0.401 ± 0.007	0.389 ± 0.009
Keggdirected	43944	20	<b>0.081 ± 0.005</b>	0.096 ± 0.007	0.088 ± 0.005
Pol	13500	26	<b>0.195 ± 0.006</b>	0.261 ± 0.008	0.3 ± 0.005
Keggundirected	57247	27	<b>0.115 ± 0.004</b>	0.126 ± 0.005	0.127 ± 0.007
Buzz	524925	77	<b>0.253 ± 0.002</b>	-	0.296 ± 0.0
Song	270000	90	<b>0.793 ± 0.004</b>	-	0.803 ± 0.004
Slice	48150	385	<b>0.049 ± 0.003</b>	0.479 ± 0.027	0.127 ± 0.001

Table 1: Test RMSE of GPs on selected UCI regression data sets. Best test RMSE for a sparse GP method is bolded.

	n	d	SoftKI-512	SVGP-512	SVGP-1024
3droad	391386	3	<b>25.159 ± 0.667</b>	29.043 ± 0.336	35.646 ± 0.492
Kin40k	36000	8	<b>2.327 ± 0.149</b>	2.792 ± 0.09	3.421 ± 0.038
Protein	41157	9	<b>2.625 ± 0.15</b>	3.03 ± 0.075	3.762 ± 0.037
Houseelectric	1844352	11	<b>118.355 ± 0.856</b>	137.845 ± 1.217	168.461 ± 1.77
Bike	15641	17	<b>0.96 ± 0.008</b>	1.224 ± 0.116	1.456 ± 0.028
Elevators	14939	18	<b>0.972 ± 0.07</b>	1.11 ± 0.005	1.383 ± 0.033
Keggdirected	43944	20	<b>2.86 ± 0.052</b>	3.233 ± 0.054	4.051 ± 0.021
Pol	13500	26	<b>0.84 ± 0.032</b>	1.039 ± 0.037	1.304 ± 0.017
Keggundirected	57247	27	<b>3.545 ± 0.098</b>	4.269 ± 0.055	5.231 ± 0.06
Buzz	524925	77	<b>37.166 ± 0.195</b>	40.015 ± 0.695	49.109 ± 0.319
Song	270000	90	<b>19.45 ± 0.203</b>	20.45 ± 0.141	25.012 ± 0.042
Slice	48150	385	<b>3.869 ± 0.044</b>	3.78 ± 0.054	4.715 ± 0.068

Table 2: Timing of hyperparameter optimization for SoftKI vs SVGP on selected UCI regression data sets. SGPR is much faster but does not support stochastic optimization.

in Figure 2.

**Accuracy.** Table 1 compares the test RMSE of various GP models trained on the UCI data set. We observe that SoftKI’s have competitive and/or more accurate test RMSE compared to SGPR or SVGP when the data dimensionality is modest (around 10). This holds on all data sets that we have tested. For low-dimensional datasets such as 3droad, SoftKI performs poorly. SKI performs well on these low-dimensional datasets.

**Timing.** Table 2 compares the average training time per epoch in seconds to for hyperparameter optimization of SoftKI vs SVGP. We do not include SGPR since it is much faster but does not support batched stochastic optimization, and thus, is limited to smaller datasets. We observe that SVGP and SoftKI have similar performance characteristics due to the mini-batch gradient descent approach that both SVGP and SoftKI

employ. SVGP requires slightly more compute since it additionally learns the parameters of a variational Gaussian distribution. We include both 512 and 1024 inducing points for SVGP for a fair timing comparison with SoftKI, although the test RMSE performance for SVGP is better with 1024 inducing points.

## 5.2 High-Dimensional Molecule Dataset

Since SoftKI’s are performant on large dimensional data sets from the UCI repository, we also test the performance on molecular potential energy surface data. These datasets have high dimensionality.

**Dataset details.** The MD22 (Chmiela et al., 2023) data set consists of biomolecules ranging from 42 atoms to 370 atoms and their properties. More concretely, we have a labeled data set  $\{(x_i, y_i)\}_i$  where  $x_i$  encodes the *Cartesian coordinates* of the atomic nuclei in the bio-molecule in Ångström’s and  $y_i$  encodes

	n	d	SoftKI-512	SGPR-512	SVGP-1024
Ac-ala3-nhme	76598	126	<b>0.67 ± 0.006</b>	0.861 ± 0.006	0.859 ± 0.005
Dha	62777	168	<b>0.592 ± 0.004</b>	0.899 ± 0.012	0.902 ± 0.011
Stachyose	24544	261	<b>0.372 ± 0.004</b>	0.68 ± 0.003	0.613 ± 0.002
At-at	18000	354	<b>0.459 ± 0.012</b>	0.594 ± 0.011	0.644 ± 0.012
At-at-cg-cg	9137	354	<b>0.398 ± 0.006</b>	0.595 ± 0.03	0.569 ± 0.039
Buckyball-catcher	5491	444	<b>0.245 ± 0.017</b>	0.776 ± 0.011	0.468 ± 0.048
Double-walled-nanotube	4528	1110	<b>0.105 ± 0.004</b>	1.001 ± 0.048	0.518 ± 0.036

Table 3: Performance of GPs on selected molecules.

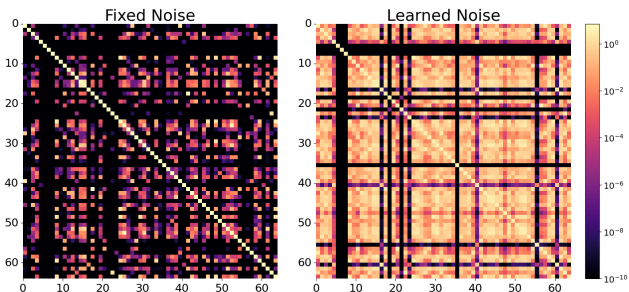
the energy of the bio-molecule in kcal/mol. The dimensionality of  $x_i$  is  $d = 3A$  where  $A$  is the number of atoms in the bio-molecule since each atom takes 3 coordinates to describe in  $3D$ -space. For example, a 42 atom system will have  $d = 126$ . We consider all available molecules.

**Experiment details.** For consistency, we keep the experimental setup the same as for UCI regression. In particular, we still use the RBF kernel and not a molecule-specific kernel that incorporates additional information such as the atomic number of each atom (*e.g.*, a Hydrogen atom) or invariances (*e.g.*, rotational invariance). We standardize the data set to have mean 0 and standard deviation 1. We note that in an actual application of GP regression to this setting, we may only opt to center the targets to be mean 0. This is because energy is a relative number that can be arbitrarily shifted, whereas scaling the distances between atoms will affect the physics.

**Accuracy.** Table 3 compares the test RMSE of various GP models trained on MD22. We see that SoftKI is by far the most performant approximate GP method. GPs that fit forces have been successfully applied to fit such data sets to chemical accuracy. In our case, we do not fit derivative information. It would be an interesting direction of future work to extend SoftKI to handle derivatives. Notably, GP regression with derivative information results in  $\mathcal{O}(n^2 d^2)$  covariance matrices, posing additional scaling challenges with  $n$  and  $d$ .

### 5.3 The Role of the Noise Hyperparameter

The noise hyper parameter  $\beta^2$  is typically learned jointly with the other GP hyper parameters when performing GP regression. However, in our experience we achieve lower RMSE by fixing  $\beta^2$  to a small value instead, *e.g.*,  $\beta^2 = 10^{-3}$ . We hypothesize that this is because a learned noise parameter can interfere with learning the locations of the inducing points. In Figure 3, we show the log entries of  $\mathbf{K}_{zz}$  for keggdirected ( $d = 20$ ). We see that the fixed noise kernel has smaller


 Figure 3: Comparison of log scaled entries of  $\mathbf{K}_{zz}$  for fixed noise versus learned noise on the  $d = 20$  keggdirected dataset.

entries compared to the kernel with learned noise. A smaller  $k(z_i, z_j)$  entry means that a pair of inducing points  $z_i$  and  $z_j$  are more dissimilar for fixed noise kernels compared to kernels with learned noise. In other words, they are further apart in data space w.r.t. the kernel. Since we seek to learn optimal placements for a set of inducing points this behavior can be understood as inducing points independently mapping the data space instead of clustering together. We observe that the gap in performance diminishes as the dimensionality increases. This matches our understanding of distances in high-dimensional spaces which are larger, and thus, more dissimilar. For additional details on the RMSE impact of learning noise, as well as the effect of increasing or decreasing the total number of inducing points used in SoftKI (see Appendix B.2 and Appendix B.4).

## 6 Conclusion

In this paper, we introduce SoftKI designed for GP regression on large and high-dimensional datasets. SoftKI combines aspects of SKI and inducing points methods to retain the benefits of kernel interpolation while also scaling to higher dimensional datasets. We have tested SoftKI on a variety of datasets from the UCI repository and shown that it outperforms other scalable GP methods. We have also demonstrated the

superior performance of SoftKI on molecular data, a high-dimensional dataset.

**Acknowledgements** Chris Camaño acknowledges support by the National Science Foundation Graduate Research Fellowship under Grant No. 2139433. Additionally, we would like to extend our appreciation to Ethan N. Epperly for his thoughtful comments and advice on this work.

## References

- Adams, A., Baek, J., and Davis, M. (2010). Fast high-dimensional filtering using the permutohedral lattice. *Comput. Graph. Forum*, 29:753–762.
- Chmiela, S., Vassilev-Galindo, V., Unke, O. T., Kabylda, A., Sauceda, H. E., Tkatchenko, A., and Müller, K.-R. (2023). Accurate global machine learning force fields for molecules with hundreds of atoms. *Science Advances*, 9(2):eadf0873.
- Foster, L., Waagen, A., Aijaz, N., Hurley, M., Luis, A., Rinsky, J., Satyavolu, C., Way, M. J., Gazis, P., and Srivastava, A. (2009). Stable and efficient gaussian process calculations. *Journal of Machine Learning Research*, 10(31):857–882.
- Gardner, J. R., Pleiss, G., Bindel, D., Weinberger, K. Q., and Wilson, A. G. (2021). Gpytorch: Black-box matrix-matrix gaussian process inference with gpu acceleration.
- Gardner, J. R., Pleiss, G., Wu, R., Weinberger, K. Q., and Wilson, A. G. (2018). Product kernel interpolation for scalable gaussian processes.
- Gibbs, M. N. and MacKay, D. J. C. (1996). Efficient implementation of Gaussian processes for interpolation.
- Girard, A. (1989). A fast ‘monte-carlo cross-validation’ procedure for large least squares problems with noisy data. *Numer. Math.*, 56(1):1–23.
- Hensman, J., Fusi, N., and Lawrence, N. D. (2013). Gaussian processes for big data. *arXiv preprint arXiv:1309.6835*.
- Hutchinson, M. (1989). A stochastic estimator of the trace of the influence matrix for laplacian smoothing splines. *Communication in Statistics- Simulation and Computation*, 18:1059–1076.
- Kapoor, S., Finzi, M., Wang, K. A., and Wilson, A. G. G. (2021). Skiing on simplices: Kernel interpolation on the permutohedral lattice for scalable gaussian processes. In *International Conference on Machine Learning*, pages 5279–5289. PMLR.
- Kelly, M., Longjohn, R., and Nottingham, K. (2017). The uci machine learning repository. <https://archive.ics.uci.edu>.
- Keys, R. (1981). Cubic convolution interpolation for digital image processing. *IEEE Transactions on Acoustics, Speech, and Signal Processing*, 29(6):1153–1160.
- Kingma, D. P. and Ba, J. (2014). Adam: A method for stochastic optimization. *arXiv preprint arXiv:1412.6980*.
- Maddox, W. J., Potapczynski, A., and Wilson, A. G. (2022). Low-precision arithmetic for fast gaussian processes. In *Uncertainty in Artificial Intelligence*, pages 1306–1316. PMLR.
- Quinonero-Candela, J. and Rasmussen, C. E. (2005). A unifying view of sparse approximate gaussian process regression. *The Journal of Machine Learning Research*, 6:1939–1959.
- Rasmussen, C. E. and Williams, C. K. I. (2005). *Gaussian Processes for Machine Learning (Adaptive Computation and Machine Learning)*. The MIT Press.
- Smola, A. and Bartlett, P. (2000). Sparse greedy gaussian process regression. In Leen, T., Dietterich, T., and Tresp, V., editors, *Advances in Neural Information Processing Systems*, volume 13. MIT Press.
- Snelson, E. and Ghahramani, Z. (2005). Sparse gaussian processes using pseudo-inputs. *Advances in neural information processing systems*, 18.
- Titsias, M. (2009). Variational learning of inducing variables in sparse gaussian processes. In *Artificial intelligence and statistics*, pages 567–574. PMLR.
- Wang, K. A., Pleiss, G., Gardner, J. R., Tyree, S., Weinberger, K. Q., and Wilson, A. G. (2019). Exact gaussian processes on a million data points.
- Williams, C. K. I. and Seeger, M. (2000). Using the nyström method to speed up kernel machines. In *Proceedings of the 13th International Conference on Neural Information Processing Systems, NIPS’00*, page 661–667, Cambridge, MA, USA. MIT Press.
- Wilson, A. and Nickisch, H. (2015). Kernel interpolation for scalable structured gaussian processes (kiss-gp). In *International conference on machine learning*, pages 1775–1784. PMLR.
- Wilson, A. G. (2014). *Covariance kernels for fast automatic pattern discovery and extrapolation with Gaussian processes*. PhD thesis, University of Cambridge Cambridge, UK.

Yadav, M., Sheldon, D., and Musco, C. (2023). Kernel interpolation with sparse grids.

## A SoftKI Posterior Predictive Derivation

We first recall how to apply the matrix inversion lemma to the posterior mean of a GP.

**Lemma A.1** (Matrix inversion with GPs).

$$\mathbf{K}_{*z}(\mathbf{K}_{zz} + \mathbf{K}_{zx}\mathbf{\Lambda}^{-1}\mathbf{K}_{xz})^{-1}\mathbf{K}_{zx}\mathbf{\Lambda}^{-1} = \mathbf{Q}_{*x}^z(\mathbf{Q}_{xx}^z + \mathbf{\Lambda})^{-1} \quad (31)$$

*Proof.*

$$\begin{aligned} \mathbf{Q}_{xx}^z + \mathbf{\Lambda} &= \mathbf{Q}_{xx}^z + \mathbf{\Lambda} && \text{(identity)} \\ \iff \mathbf{I} &= (\mathbf{Q}_{xx}^z + \mathbf{\Lambda})^{-1}\mathbf{Q}_{xx}^z + (\mathbf{Q}_{xx}^z + \mathbf{\Lambda})^{-1}\mathbf{\Lambda} && \text{(mult by } (\mathbf{Q}_{xx}^z + \mathbf{\Lambda})^{-1}\text{)} \\ \iff \mathbf{I} - (\mathbf{Q}_{xx}^z + \mathbf{\Lambda})^{-1}\mathbf{Q}_{xx}^z &= (\mathbf{Q}_{xx}^z + \mathbf{\Lambda})^{-1}\mathbf{\Lambda} && \text{(rearrange)} \\ \iff \mathbf{Q}_{*x}^z - \mathbf{Q}_{*x}^z(\mathbf{Q}_{xx}^z + \mathbf{\Lambda})^{-1}\mathbf{Q}_{xx}^z &= \mathbf{Q}_{*x}^z(\mathbf{Q}_{xx}^z + \mathbf{\Lambda})^{-1}\mathbf{\Lambda} && \text{(mult both sides by } \mathbf{Q}_{*x}^z \text{ on left)} \\ \iff \mathbf{K}_{*z}\mathbf{K}_{zz}^{-1}\mathbf{K}_{zx} - \mathbf{K}_{*z}\mathbf{K}_{zz}^{-1}\mathbf{K}_{zx}(\mathbf{K}_{xz}\mathbf{K}_{zz}^{-1}\mathbf{K}_{zx} + \mathbf{\Lambda})^{-1}\mathbf{K}_{xz}\mathbf{K}_{zz}^{-1}\mathbf{K}_{zx} &= \mathbf{Q}_{*x}^z(\mathbf{Q}_{xx}^z + \mathbf{\Lambda})^{-1}\mathbf{\Lambda} && \text{(defn } \mathbf{Q}_{xx}^z\text{)} \\ \iff \mathbf{K}_{*z}(\mathbf{K}_{zz}^{-1} - \mathbf{K}_{zz}^{-1}\mathbf{K}_{zx}(\mathbf{K}_{xz}\mathbf{K}_{zz}^{-1}\mathbf{K}_{zx} + \mathbf{\Lambda})^{-1}\mathbf{K}_{xz}\mathbf{K}_{zz}^{-1})\mathbf{K}_{zx} &= \mathbf{Q}_{*x}^z(\mathbf{Q}_{xx}^z + \mathbf{\Lambda})^{-1}\mathbf{\Lambda} && \text{(factor)} \\ \iff \mathbf{K}_{*z}(\mathbf{K}_{zz} + \mathbf{K}_{zx}\mathbf{\Lambda}^{-1}\mathbf{K}_{xz})^{-1}\mathbf{K}_{zx} &= \mathbf{Q}_{*x}^z(\mathbf{Q}_{xx}^z + \mathbf{\Lambda})^{-1}\mathbf{\Lambda} && \text{(matrix inversion lemma)} \\ \iff \mathbf{K}_{*z}(\mathbf{K}_{zz} + \mathbf{K}_{zx}\mathbf{\Lambda}^{-1}\mathbf{K}_{xz})^{-1}\mathbf{K}_{zx}\mathbf{\Lambda}^{-1} &= \mathbf{Q}_{*x}^z(\mathbf{Q}_{xx}^z + \mathbf{\Lambda})^{-1}. && \text{(mult } \mathbf{\Lambda}^{-1} \text{ on right)} \end{aligned}$$

□

Now, we extend the matrix inversion lemma to SoftKI.

**Lemma A.2** (Matrix inversion with interpolation).

$$\hat{\mathbf{K}}_{*z}(\mathbf{K}_{zz} + \hat{\mathbf{K}}_{zx}\mathbf{\Lambda}^{-1}\hat{\mathbf{K}}_{xz})^{-1}\hat{\mathbf{K}}_{zx}\mathbf{\Lambda}^{-1} = \tilde{\mathbf{Q}}_{*x}^z(\tilde{\mathbf{Q}}_{xx}^z + \mathbf{\Lambda})^{-1} \quad (32)$$

*Proof.* Recall  $\tilde{\mathbf{Q}}_{xx}^z = \mathbf{W}_{xz}\mathbf{K}_{zz}\mathbf{W}_{zx} = \mathbf{W}_{xz}\mathbf{K}_{zz}\mathbf{K}_{zz}^{-1}\mathbf{K}_{zz}\mathbf{W}_{zx} = \hat{\mathbf{K}}_{xz}\mathbf{K}_{zz}^{-1}\hat{\mathbf{K}}_{zx}$ . The result follows by applying Lemma A with  $\mathbf{K}_{xz}$  replaced with  $\hat{\mathbf{K}}_{xz}$ . □

## B Additional Experiments

In this section, we examine the influence of various aspects of the SoftKI model and its sensitivity to algorithm design decisions made throughout the paper.

In Section B.1, we discuss the rationale behind using a stochastic trace estimation scheme for computing the marginal log likelihood during stochastic optimization. Sections B.2 and B.4 provide further insights into the model's dependence on the noise hyperparameter and the effect of the number of inducing points. Lastly, B.3 motivates choice of linear solver, comparing the use alternative linear solvers for the posterior inference procedure described in. Section 4.3.

### B.1 Effect of Hutchinson Pseudoloss

In Section 4.2, we advocate for the use of the Hutchinson pseudoloss to overcome numerical stability issues that arise when calculating the exact marginal log likelihood. This adjustment is specifically to address situations where the matrix  $\tilde{\mathbf{Q}}_{xx}^z + \mathbf{\Lambda}$  is not psd. In other approximate GP model using `gpytorch`, this challenge is typically met by performing a Cholesky decomposition followed by an efficient low-rank computation of the log determinant through the matrix determinant lemma. In our experience even when using versions of the Cholesky decomposition that add additional jitter along the diagonal there are still situations where  $\tilde{\mathbf{Q}}_{xx}^z + \mathbf{\Lambda}$  can be poorly conditioned. The Hutchinson pseudoloss offers a more stable alternative because it does not rely on the matrix being positive semi-definite.

In Table 4 we replicate the UCI experiment of Section 5.1 using the Hutchinson pseudoloss  $\log \tilde{p}(\mathbf{y}; \theta)$  and the exact marginal log likelihood  $\log p(\mathbf{y}; \theta)$ . For most situations the exact marginal log likelihood produces a lower

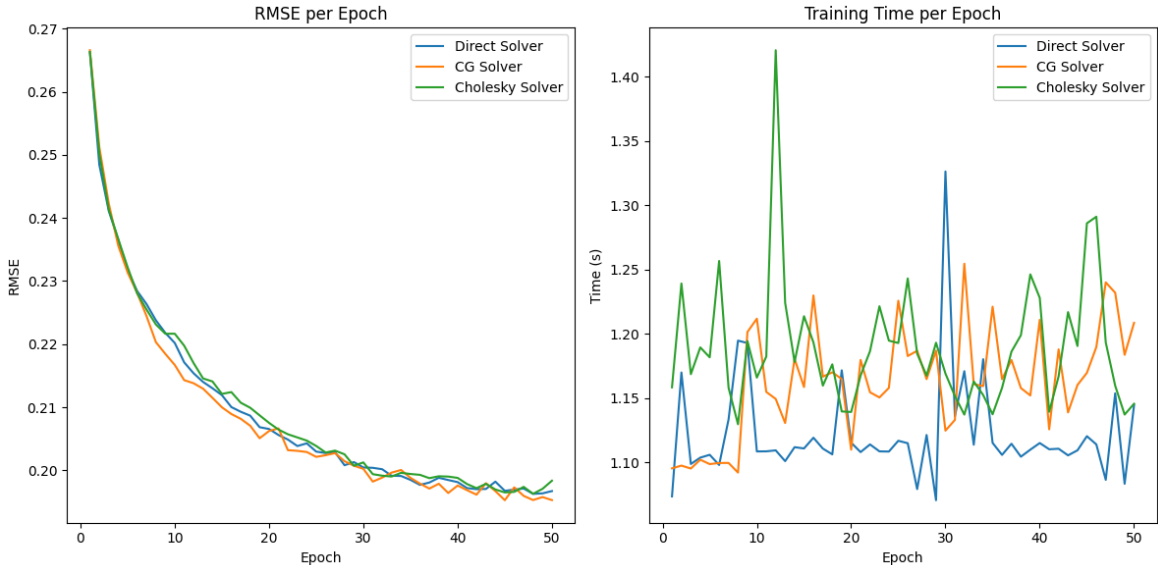


Figure 4: Comparison of linear solver choices during pseudoloss computation and their impact on final model accuracy for the Po1 dataset.

	N	D	$\log \tilde{p}(\mathbf{y}; \theta)$	$\log p(\mathbf{y}; \theta)$
3droad	391386	3	<b>0.605</b> $\pm$ <b>0.0</b>	-
Kin40k	36000	8	<b>0.237</b> $\pm$ <b>0.008</b>	0.24 $\pm$ 0.0
Protein	41157	9	<b>0.649</b> $\pm$ <b>0.01</b>	-
Houseelectric	1844352	11	<b>0.064</b> $\pm$ <b>0.001</b>	-
Bike	15641	17	0.204 $\pm$ 0.006	<b>0.203</b> $\pm$ <b>0.006</b>
Elevators	14939	18	<b>0.389</b> $\pm$ <b>0.01</b>	<b>0.389</b> $\pm$ <b>0.01</b>
Keggdirected	43944	20	<b>0.081</b> $\pm$ <b>0.005</b>	<b>0.081</b> $\pm$ <b>0.005</b>
Po1	13500	26	0.195 $\pm$ 0.006	<b>0.193</b> $\pm$ <b>0.006</b>
Keggundirected	57247	27	<b>0.115</b> $\pm$ <b>0.004</b>	-
Buzz	524925	77	0.254 $\pm$ 0.0	<b>0.248</b> $\pm$ <b>0.001</b>
Song	270000	90	<b>0.793</b> $\pm$ <b>0.005</b>	<b>0.793</b> $\pm$ <b>0.004</b>
Slice	48150	385	0.049 $\pm$ 0.003	<b>0.024</b> $\pm$ <b>0.005</b>

Table 4: Effect on SoftKI RMSE using  $\log \tilde{p}(\mathbf{y}; \theta)$  vs. standard  $\log p(\mathbf{y}; \theta)$ .

test RMSE result than the Hutchinson pseudoloss, however for some datasets that produce noisy  $\tilde{\mathbf{Q}}_{\mathbf{x}\mathbf{x}}^z + \mathbf{\Lambda}$  the method can crash due to the Cholesky decomposition failing.

Hutchinson pseudoloss involves computing solutions to the equations

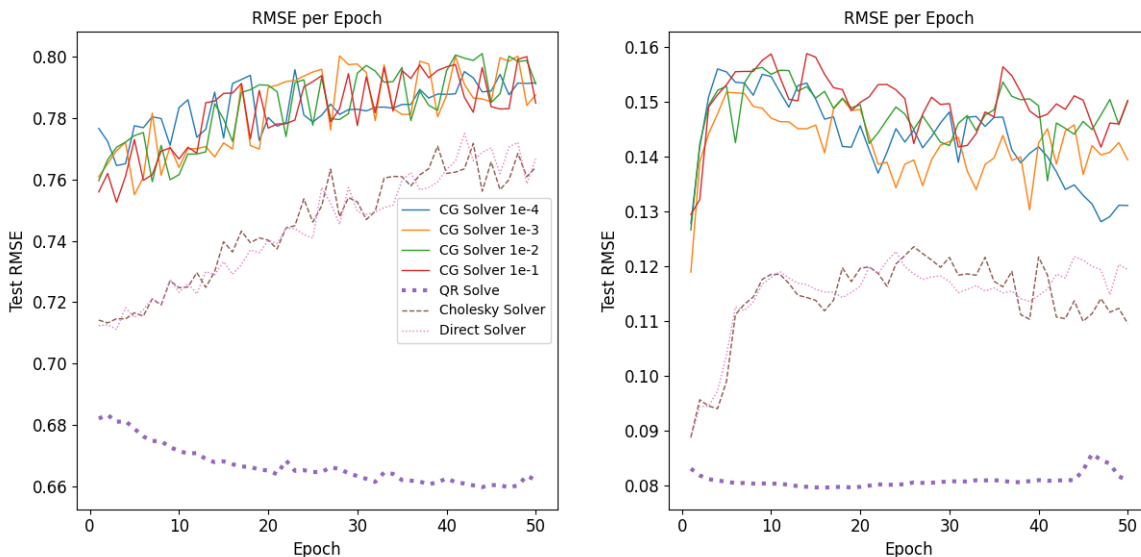
$$\Sigma_{\theta}(\mathbf{b}_0, \mathbf{b}_1, \dots, \mathbf{b}_n) = (\mathbf{y}, \mathbf{a}_1, \dots, \mathbf{a}_M),$$

where  $\Sigma_{\theta}$  is the covariance matrix parameterized by GP hyperparameters  $\theta$ ,  $\mathbf{y}$  is the target vector, and  $\mathbf{a}_i$  are unit length normalized Gaussian random vectors. In most implementations, these systems are typically solved using CG solvers due to their efficiency with large, sparse systems. However, during the training of a SoftKI, the matrices involved are relatively small because of the mini-batching strategy employed (See Algorithm 1). This makes direct solvers more efficient and attractive in practice. Figure 4 illustrates the impact of different linear solvers for this task, comparing CG, a direct solver, and a Cholesky decomposition routine.

In this example, we set the tolerance of the CG solver to  $10^{-4}$  to achieve accuracy comparable to that of a direct solve. Following the approach outlined by Gardner et al. (Gardner et al., 2021), we employ a rank-10 pivoted Cholesky preconditioner. Additionally, we incorporate the CG stabilization modifications proposed by Maddox et al in (Maddox et al., 2022). All three approaches exhibited roughly similar behavior, with the direct solver

	N	D	$\beta^2 = 0.001$	Learn $\beta^2$
3droad	391386	3	<b>0.605</b> $\pm$ <b>0.0</b>	0.728 $\pm$ 0.001
Kin40k	36000	8	<b>0.237</b> $\pm$ <b>0.008</b>	0.385 $\pm$ 0.004
Protein	41157	9	<b>0.649</b> $\pm$ <b>0.01</b>	0.725 $\pm$ 0.004
Houseelectric	1844352	11	<b>0.064</b> $\pm$ <b>0.001</b>	0.072 $\pm$ 0.001
Bike	15641	17	<b>0.204</b> $\pm$ <b>0.006</b>	0.245 $\pm$ 0.002
Elevators	14939	18	<b>0.389</b> $\pm$ <b>0.01</b>	0.393 $\pm$ 0.005
Keggdirected	43944	20	<b>0.081</b> $\pm$ <b>0.005</b>	0.083 $\pm$ 0.005
Pol	13500	26	<b>0.195</b> $\pm$ <b>0.006</b>	0.235 $\pm$ 0.006
Keggundirected	57247	27	<b>0.115</b> $\pm$ <b>0.004</b>	0.118 $\pm$ 0.004
Buzz	524925	77	<b>0.254</b> $\pm$ <b>0.0</b>	0.262 $\pm$ 0.004
Song	270000	90	0.793 $\pm$ 0.005	<b>0.791</b> $\pm$ <b>0.005</b>
Slice	48150	385	<b>0.049</b> $\pm$ <b>0.003</b>	0.051 $\pm$ 0.003

Table 5: SoftKI test RMSE with fixed noise and learned noise.

Figure 5: Test RMSE of SoftKI models trained using different linear solvers on the `keggundirected` dataset (*left*) and the `protein` dataset (*right*).

running slightly faster than the alternatives. We suspect this performance gain is due to low-level optimizations in the underlying numerical linear algebra package used for direct linear solves.

## B.2 Additional Experiments for the Noise Hyperparameter

As we discussed in Section 5.3, the noise hyperparameter plays a delicate role in the performance of a SoftKI. Earlier we argued that allowing the noise hyperparameter to be learned jointly with other hyperparameters can negatively affect the final test RMSE of the model. To investigate this further, we revisited the UCI benchmark, this time treating the noise as a learnable parameter, while keeping all other settings aligned with the original experiment setting. The results, summarized in Table 5, demonstrate that for most datasets allowing the model to learn the noise negatively impacts the the final RMSE.

## B.3 Alternative Methods for Posterior Inference

Section 4.3 details the adaptation of the QR stabilized linear solve for approximate kernels (Foster et al., 2009) to the SoftKI setting. In this section, we provide empirical evidence illustrating how other linear solvers fail when

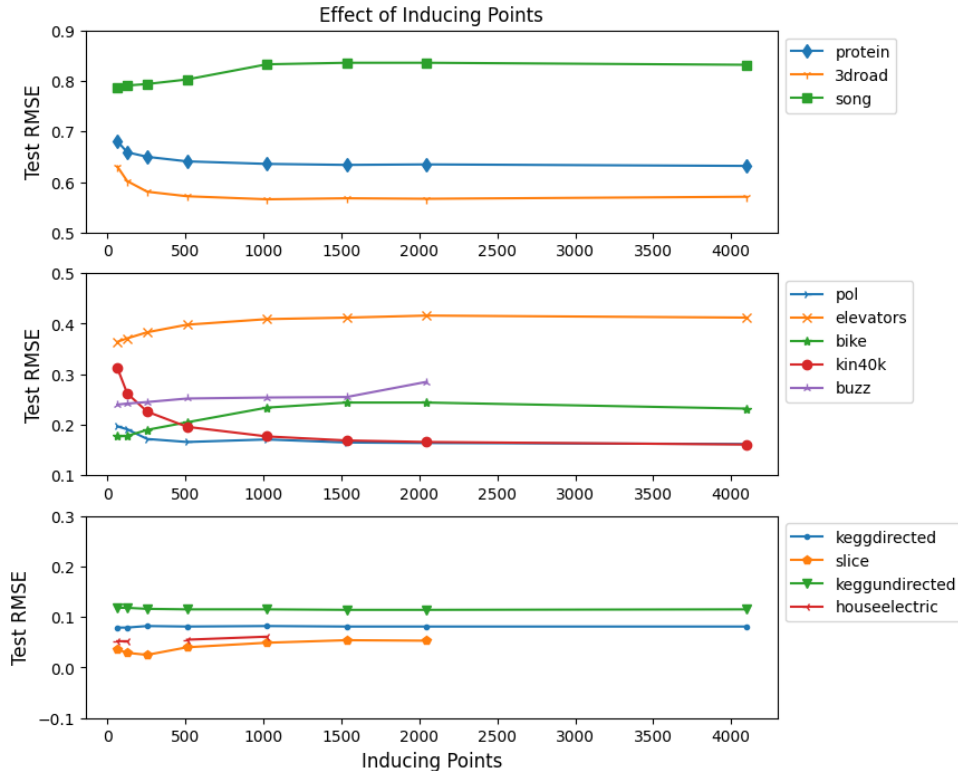


Figure 6: Effect of increasing the number of inducing points for a SoftKI for the UCI datasets.

confronted with datasets that generate noisy kernels. We focus on two datasets, `protein` and `keggundirected`, which have previously caused instability in the Hutchinson pseudoloss computation.

As a reminder the QR stabilized linear solve is motivated by the challenge of solving the linear system:

$$\hat{\mathbf{C}} \boldsymbol{\alpha} = \hat{\mathbf{K}}_{\mathbf{z}\mathbf{x}} \boldsymbol{\Lambda}^{-1} \mathbf{y}, \quad (33)$$

where  $\hat{\mathbf{C}}$  is the estimated (potentially noisy) kernel matrix  $\hat{\mathbf{C}} = \mathbf{K}_{\mathbf{z}\mathbf{z}} + \hat{\mathbf{K}}_{\mathbf{z}\mathbf{x}} \boldsymbol{\Lambda}^{-1} \hat{\mathbf{K}}_{\mathbf{x}\mathbf{z}}$ , and  $\hat{\mathbf{K}}_{\mathbf{x}\mathbf{z}} = \mathbf{W}_{\mathbf{x}\mathbf{z}} \mathbf{K}_{\mathbf{z}\mathbf{z}}$  is the interpolated kernel between inducing points  $\mathbf{z}$  and training points  $\mathbf{x}$ .

In this example we evaluate a direct solver, the Cholesky decomposition method, and CG with convergence tolerances set to  $1 \times 10^{-1}$ ,  $1 \times 10^{-2}$ ,  $1 \times 10^{-3}$ , and  $1 \times 10^{-4}$ . Despite adjusting the tolerances for the CG method, our experiments revealed that all solvers—except for the QR-stabilized routine—resulted in training instability. Figure 5 depicts the test RMSE performance across the different solvers. The direct and Cholesky solvers, while more stable than the CG solvers, failed to produce reliable solutions. Similarly, the CG method did not converge to acceptable solutions within the tested tolerance levels. In contrast, the QR-stabilized solver consistently produced stable and accurate solutions justifying its choice as a correctional measure that stabilizes a SoftKI on difficult problems.

#### B.4 The Effect of Inducing Points

Figure 3 illustrates the effect of the number of inducing points on the test RMSE of SoftKI. We find that increasing the number of inducing points is helpful for improving test RMSE performance on some datasets (*e.g.*, `kin40k` and `pol`) while it is detrimental for other datasets (*e.g.*, `elevators` and `bike`). While it would stand to reason that increasing the number of inducing points would improve performance (up to a certain point), it is not clear to us why increasing the number of inducing points would be detrimental in some cases. We do not observe over fitting in the test RMSE curves but see saturation at a higher test RMSE. It would be an interesting direction of future work to investigate this phenomenon and how to improve it.